Role of interfaces in the magnetoresistance of Au/Fe/Au/Fe multilayers

P. Weinberger, J. Zabloudil, and R. H. Hammerling
Center for Computational Materials Science, Technical University Vienna, Vienna, Austria

L. Szunyogh
Department of Theoretical Physics, Budapest University of Technology, Budafoki út 8, H-1521, Budapest, Hungary
and Center for Computational Materials Science, Technical University Vienna, Vienna, Austria

T. L. Monchesky and B. Heinrich
Physics Department, Simon-Fraser University, 8888 University Drive, Burnaby, BC, Canada V5A 1S6
(Received 10 July 2002; published 6 February 2003)

By using the fully relativistic spin-polarized screened Korringa-Kohn-Rostoker method and the corresponding Kubo-Greenwood equation resistivities and the giant magnetoresistance are evaluated for Fe/Au/Fe/Au spin valves assuming both bcc-like Fe and fcc-Au leads. The theoretically obtained values for a spacer thickness of 7 monolayers of Au are in a rather good agreement with the corresponding experimental data. These data, in particular the temperature dependence of the resistivities reported in here, are analyzed with respect to the experimental setup and related to the theoretical models assumed. Since in the theoretical calculations interdiffused interfaces are taken into account by means of the inhomogeneous coherent potential approximation, the role of the interfaces in the magnetoresistance of this system can be discussed rigorously.

DOI: 10.1103/PhysRevB.67.054404 PACS number(s): 75.30.Gw, 75.70.Ak, 75.70.Cn

I. INTRODUCTION

In a very recent investigation Enders *et al.*[1] carried out electric transport measurements in the current in-plane geometry (CIP) for the system $Au_{20}Fe_{10}Au_7Fe_{28}$/GaAs(100) in comparison with a study of the layer dependence of the conductivity of Fe (x Å)/GaAs(100) and Au (x Å)Fe (40 Å)/GaAs(100) with x varying between 0 and 600 Å. In this study, not only is the GMR value for the spin valve $Au_{20}Fe_{10}Au_7Fe_{28}$/GaAs(100) given but also the conductivities in the parallel and the antiparallel alignment. It is tempting to carry out corresponding truly *ab initio* electric transport calculations, in particular since these authors also tried to present a ''parametric'' model to explain their experimental results. The actual values for the resistivities allow a direct comparison of experimental and theoretical results, since quoting only ratios thereof prevent a detailed discussion of the various circumstances that enter both the experimental and the theoretical setups. Unfortunately from the paper by Enders *et al.* very little can be said about the actual structure of the spin-valve system, although a rather detailed study of the roughness in terms of scanning tunnel microscope (STM) images was carried out. Since in this system the left Au and the right Fe slab are quite thick and the GaAs substrate can be replaced by a vacuum barrier, the question arises which of the two slabs can be considered as the electron reservoir, i.e., can be assumed to be a semi-infinite system that determines the Fermi energy. In here both (theoretical) limiting cases are considered, namely a bcc-Fe(100) substrate and a fcc-Au(100) substrate.

In the first section the experimental setup is presented, in Sec. II the theoretical and computational details are briefly summarized, followed by a presentation and discussion of the theoretical results.

II. EXPERIMENTAL SETUP

The sample was grown on semi-insulating GaAs(001). The GaAs surface was prepared in ultrahigh vacuum by removing the oxide from epi-ready wafers with 500 eV Ar^+. The sample temperature was gradually raised under reflection high-energy electron diffraction (RHEED) observation until a well ordered (4×6) reconstruction was obtained at a temperature of roughly 600 °C. Fe was evaporated on room-temperature GaAs in a base pressure of 1×10^{-10} Torr at a rate of roughly 1 Å/min as measured by RHEED intensity oscillations and a quartz microbalance. Once a thickness of 20 monolayers (ML's) (28.7 Å) was grown, the ML of As that segregated to the surface of Fe was removed with 500-eV Ar^+. Fe was then grown on the As-free surface at a substrate temperature of 200 °C in order to improve the surface quality until the Fe film reached a thickness of 28 ML's. A 7-ML (14.3 Å) Au film was evaporated at a rate of 2 Å/min onto the Fe surface, once the sample had cooled to room temperature. This was followed by the deposition of 10-ML Fe film and finally a 20-ML Au cap to protect the multilayer from oxidation. For details of the growth and the magnetic properties of the multilayer, see Refs. 2 and 3.

Once the sample had been grown, it was removed from vacuum and patterned using photolithography. A 2-μm-thick photoresist was spun and developed. The photoresist served as a mask while undesired portions of the film were sputtered away with 3-keV Ar^+ leaving a pattern consisting of four 1.5-mm^2 contact pads connected to the 0.5×1.0-mm^2 region where the resistance was measured. To make electrical contact to the film, In wires were pressed into the Au cap of the four contact pads. Four-probe resistance measurements were preformed in a liquid-helium close cycle cooler cryostat from 300 K down to 10 K.

TABLE I. Investigated systems.

System A 2-ML interdiffusion at two Fe/Au interfaces	System B 2-ML interdiffusion at all Fe/Au interfaces	System C 2-ML interdiffusion at all Fe/Au interfaces
bcc-Fe(100)	bcc-Fe(100)	fcc-Au(100)
Fe_{11}	Fe_{11}	Au_5
$[Fe_cAu_{1-c}]$	$[Fe_cAu_{1-c}]$	$[Au_cFe_{1-c}]$
$[Au_cFe_{1-c}]$	$[Au_cFe_{1-c}]$	$[Fe_cAu_{1-c}]$
Au_5	Au_5	Fe_8
$[Au_cFe_{1-c}]$	$[Au_cFe_{1-c}]$	$[Fe_cAu_{1-c}]$
$[Fe_cAu_{1-c}]$	$[Fe_cAu_{1-c}]$	$[Au_cFe_{1-c}]$
Fe_9	Fe_8	Au_5
Au_5	$[Fe_cAu_{1-c}]$	$[Au_cFe_{1-c}]$
vac	$[Au_cFe_{1-c}]$	$[Fe_cAu_{1-c}]$
	Au_4	Fe_{10}
	vac	vac

III. THEORETICAL AND COMPUTATIONAL DETAILS

A. Self-consistent calculations

The fully relativistic spin-polarized screened Korringa-Kohn-Rostoker method for layered systems[4] is applied to calculate the electronic structure and magnetic properties of the systems listed in Table I. In all calculations either a bcc-Fe (lattice spacing of 5.27 a.u.) or a fcc-Au (lattice spacing of 7.6813 a.u.) parent lattice[5] is assumed, i.e., no layer relaxation is considered. It should be recalled that, e.g., in the case of a bcc-Fe parent lattice the planes of sites in a bcc lattice with the lattice spacing of bulk Fe are decorated with Fe atoms (left semi-infinite system, bulk part of the system), a few planes of Fe atoms serving as buffer to the bulk, planes of atoms forming the multilayer part of the system (planes of Fe or Au atoms) and empty planes (right semi-infinite system, vacuum part of the system). In the case of a fcc-Au parent lattice a fcc lattice with the lattice spacing of bulk Au is decorated with Au, Fe, and empty planes. In principle the distance between the planes can be different,[6] the in-plane lattice constant, however, has to be the same in all planes, since the use of two-dimensional lattice Fourier transformations requires one and the same two-dimensional translational group in all atomic layers. Clearly enough a bcc-Fe parent lattice differs substantially from a fcc-Au parent lattice (interlayer distance, in-plane lattice constant, different two-dimensional lattice). It is important to keep a very clear language in dealing with multilayer systems and/or free surfaces of solids since by definition the term fcc or bcc refers to an infinite system (no surface) in which all atoms are identical!

A metallic semi-infinite system (substrate) is needed to pinpoint the Fermi energy: the substrate (lead) serves as (infinite) electron reservoir. If a free-standing film is considered—in principle the other kind of theoretical approach, then the Fermi energy is determined by the presence of two surfaces and depends on the number and type of atomic layers. Considering the actual size of the investigated system, namely 65 atomic layers on GaAs, this second kind of approach remains only a theoretical possibility.

All investigations concerning interdiffusion at the Au/Fe interfaces were carried out in terms of the (inhomogeneous) coherent potential approximation for layered systems.[7] All investigated cases are compiled in Table I; the interdiffusion concentration was varied between 0 and 20%. In Table I systems A and B refer to the case bcc-Fe(100)/$Fe_{12}Au_7Fe_{10}Au_5$Vac, i.e., to a model system in which bcc-Fe is the substrate. Note that in this model system the slab of 12 Fe layers serves as buffer to the substrate. System A takes into account interdiffusion at the Au/Fe interfaces of the Au spacer, system B at all three Au/Fe interfaces. System C represents a model system with Au as substrate (six Au layers serve as buffer), fcc-Au(100)/$Au_6Fe_{10}Au_7Fe_{11}$Vac, and interdiffusion considered at all Au/Fe interfaces. It should be noted that the inclusion of a sufficient number of buffer layers is neccessary in order to describe correctly the damping of the Friedel oscillations of the layer-resolved Madelung potentials into the semi-infinite substrate. For an illustration of such oscillations, see Fig. 5 of Ref. 8.

In order to determine self-consistently within the local-density approximation (LDA) (Ref. 9) the effective potentials and effective exchange fields for each particular system under consideration a minimum of 45 $\mathbf{k}_\parallel$ points in the irreducible wedge of the surface Brillouin zone (ISBZ) was used. All self-consistent calculations refer to a ferromagnetic configuration with the orientation of the magnetization parallel to the surface normal.

B. Magnetic anisotropy energy

Suppose $\mathcal{C}_0$ and $\mathcal{C}$ denote two different magnetic configurations, which differ in (total) energy by

$$\Delta E = E(\mathcal{C}) - E(\mathcal{C}_0), \tag{1}$$

where $\mathcal{C}_0$ usually is termed the magnetic reference configuration. Here $\mathcal{C}_0$ refers to a ferromagnetic configuration in which the magnetization in all layers is orientated along the surface normal (perpendicular to the surface). If in Eq. (1) $\mathcal{C}$ refers to a ferromagnetic configuration with a uniform in-plane orientation of the magnetization then ΔE is said to be the LDA (total) energy part of the magnetic anisotropy energy E_a, to which—in principle—also the shape anisotropy, namely the energy difference corresponding to the magnetic dipole-dipole interaction ΔE_{dd}, has to be added.[4] Since for a trilayer system with a semi-infinite magnetic lead on one side a definition of the shape anisotropy is somewhat ambiguous, here only ΔE is investigated.

The energy difference in Eq. (1) is evaluated by making use of the magnetic force theorem which implies that only the reference configuration is determined self-consistently within the local-density functional approximation and ΔE is replaced by the respective difference in the grand canonical potentials,

$$\Delta E \sim \Delta E_b = \sum_{p=1}^{n} \Delta E_b^p, \tag{2}$$

$$\Delta E_b^p = \int_{\epsilon_b}^{\epsilon_F} [n^p(\epsilon;\mathcal{C}) - n^p(\epsilon;\mathcal{C}_0)](\epsilon - \epsilon_F) d\epsilon, \tag{3}$$

which as indicated in Eq. (3) can be written at zero temperature in terms of layer-dependent quantities ΔE_b^p with n denoting the total number of layers p, $n^p(\epsilon;\mathcal{C})$ layer-resolved densities-of-states for a given magnetic configuration $\mathcal{C}$, ϵ_b the (valence) band bottom, and ϵ_F the Fermi energy of the substrate. It should be noted that according to Eq. (1) $\Delta E_b > 0$ implies that $\mathcal{C}_0$ is the energetically preferred magnetic configuration. In the present paper all ΔE_b are evaluated in terms of a contour integration in the complex energy plane at zero temperature by using a total of 990 $\mathbf{k}_\parallel$ points in the ISBZ, which—as was shown[4] in the case of magnetic anisotropy energies—guarantees well converged results.

C. Electric transport

In the case of a current-in-plane (CIP) geometry the resistivity for a layered system in a particular magnetic configuration $\mathcal{C}$ is given by[7]

$$\rho_{xx}(n;\mathbf{c};\mathcal{C}) = \lim_{\delta \to 0} \rho_{xx}(n;\mathbf{c};\mathcal{C};\delta), \tag{4}$$

where n denotes the number of layers considered, $\mathbf{c} = \{c_1, c_2, \ldots, c_n\}$ is a set containing the layerwise concentrations, δ is the imaginary part of the complex Fermi energy $\epsilon_F + i\delta$, and $\rho_{xx}(n;\mathbf{c};\mathcal{C})$ is related to the conductivity by

$$\rho_{xx}(n;\mathbf{c};\mathcal{C};\delta) = \sigma_{xx}^{-1}(n;\mathbf{c};\mathcal{C};\delta), \tag{5}$$

$$\sigma_{xx}(n;\mathbf{c};\mathcal{C};\delta) = \sum_{i,j=1}^{n} \sigma_{xx}^{ij}(n;\mathbf{c};\mathcal{C};\delta); \tag{6}$$

see also the discussions in Refs. 10–12. For practical reasons $\sigma_{xx}(n;c;C;\delta)$ can only be calculated efficiently for finite values of δ and is then numerically extrapolated (continued) to the real energy axis. For an illustration of such an extrapolation, see, e.g., Fig. 4 of Ref. 8. The (giant) magnetoresistance ratio, usually termed GMR, is then defined by

$$R(n;\mathbf{c}) = \frac{\rho_{xx}(n;\mathbf{c};\mathcal{C}) - \rho_{xx}(n;\mathbf{c};\mathcal{C}_0)}{\rho_{xx}(n;\mathbf{c};\mathcal{C})}, \tag{7}$$

where $\mathcal{C}_0$ and $\mathcal{C}$ refer to the ferro- (parallel) and antiferromagnetic (antiparallel) configuration, respectively. The advantage of this kind of definition of the GMR is simply that $R(n;\mathbf{c}) \leqslant 1$. For practical purposes it is useful to define also the below quantity:

$$R(n;\mathbf{c};\delta) = \frac{\rho_{xx}(n;\mathbf{c};\mathcal{C};\delta) - \rho_{xx}(n;\mathbf{c};\mathcal{C}_0;\delta)}{\rho_{xx}(n;\mathbf{c};\mathcal{C};\delta)}, \tag{8}$$

$$R(n;\mathbf{c};\delta) \leqslant R(n;\mathbf{c}), \tag{9}$$

since a finite δ mimics a finite (electronic) temperature and/or structural roughness. The surface Brillouin-zone integrals needed in the evaluation of the electrical conductivity within the Kubo-Greenwood approach[7] were obtained by considering 1830 $\mathbf{k}_\parallel$ points in the irreducible wedge of the surface Brillouin zone. All scattering channels up to and including $\ell_{\max} = 2$ were taken into account.

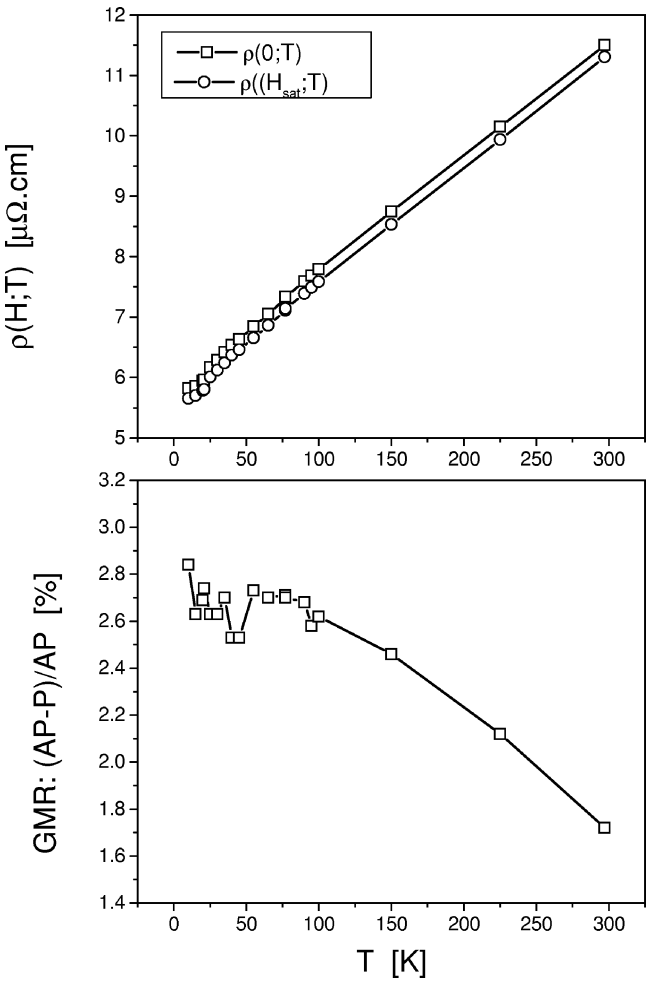

FIG. 1. Experimental field- and temperature-dependent resistivities (top) and temperature-dependent giant magnetoresistance (bottom).

From Eq. (6) for illustrative purposes layer-dependent conductivities can be defined

$$\sigma_{xx}^{i}(n;\mathbf{c};\mathcal{C};\delta) = \sum_{j=1}^{n} \sigma_{xx}^{ij}(n;\mathbf{c};\mathcal{C};\delta), \tag{10}$$

keeping in mind, however, that only the sum over these layer-dependent conductivities is well defined,

$$\sigma_{xx}(n;\mathbf{c};\mathcal{C};\delta) = \sum_{i=1}^{n} \sigma_{xx}^{i}(n;\mathbf{c};\mathcal{C};\delta). \tag{11}$$

It should be noted that in two-dimensional translationally invariant systems the double sum over all scattering sites in the Kubo-Greenwood equation can be reduced in terms of lattice Fourier transformation to a double sum over atomic layers. For further theoretical details, see Ref. 7.

IV. RESULTS

In the upper part of Fig. 1 the temperature dependence of the experimentally obtained resistivities in the parallel (zero

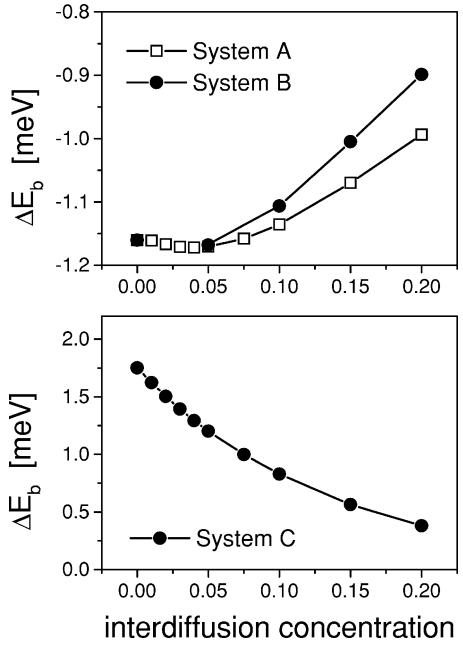

FIG. 2. Band energy contribution to the magnetic anisotropy energy in Fe/Au/Fe multilayers.

field) and the antiparallel (saturation field) alignment are shown together with the corresponding temperature (T) dependence of the giant magnetoresistance (GMR). As can be seen from this figure for $T>20$ K these resistivities vary mostly linearly with respect to T, indicating, however, a kind of flattening out for $T>10$ K. At $T=10$ K the actual values are 5.6522 and 5.8175 $\mu\Omega$ cm in the parallel and the antiparallel case, respectively. This corresponds to a GMR of 2.84%; see the definition in Eq. (7). At room temperature the values for the resistivities are roughly twice as large and lead to a GMR ratio of 1.72%. In the lower part of Fig. 1 the temperature variation of the GMR is displayed. It is obvious that for $T<70$ K the functional behavior becomes a bit rough suggesting in turn an error bar of about 0.10–0.20% for the experimental GMR values.

In Fig. 2 the band energy part of the magnetic anisotropy energy is shown versus the interdiffusion concentration c for the systems listed in Table I. As can be seen the band energy part of the magnetic anisotropy energy, ΔE_b, see Eq. (1), favors an in-plane orientation of the magnetization in the case of an Fe substrate, but a perpendicular one for the Au substrate. The top of Fig. 2 shows that interdiffusion of the third Au/Fe interface modifies ΔE_b only little. For the rather thick magnetic layers considered, however, the overall magnetization of the system most likely is in plane due to magnetostatic dipole-dipole interactions (shape anisotropy); therefore in the transport calculations the orientation of the magnetization points along the x axis (in plane).

Experimentally the exchange coupling for a 7-ML-thick Au spacer between Fe layers is said to be antiferromagnetic. The experimental finding reveals antiferromagnetic coupling through a Au spacer of thickness of 14–22 Å, below which only ferromagnetic coupling pertains. Unfortunately in the relevant figure of Fuß *et al.*[13] a second scale is introduced equating 1 ML to about 2 Å. This is the case in system C

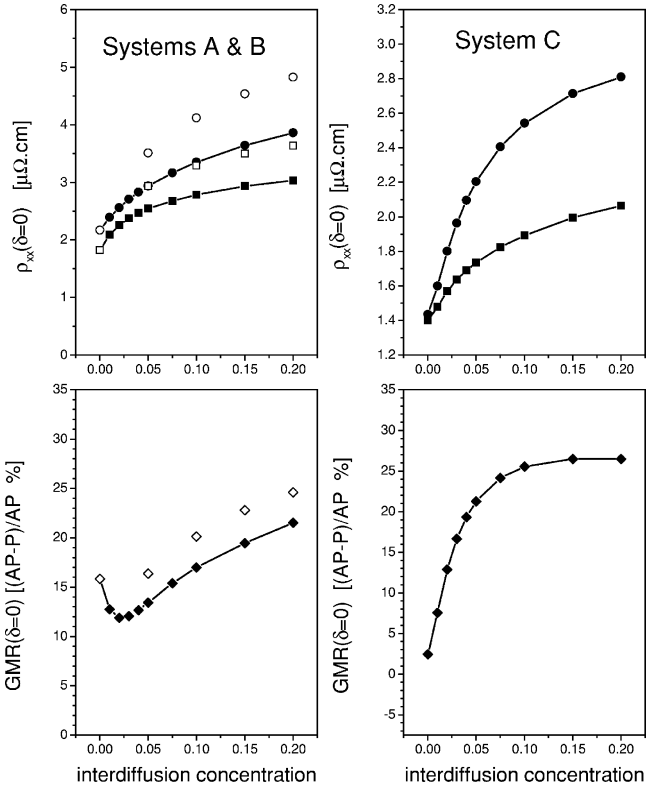

FIG. 3. CIP resistivity and GMR in Fe/Au/Fe multilayers as continued to the real axis. Squares refer to the parallel alignment, circles to the antiparallel alignment. For systems A and C full symbols apply, for system B open symbols; see also Table I.

(interlayer distance 2.03 Å), since then 7 ML's of a Au spacer refer to an actual thickness of about 14 Å. With an interlayer distance of 1.39 Å (Fe substrate) the spacer thickness amounts only to about 10 Å. This is also what corresponding calculations (not shown here) predict. Clearly enough it was not the goal of the present paper—neither experimentally nor theoretically—to study the oscillations of the interlayer exchange coupling with respect to the thickness of the Au spacer. There is a whole series of papers[14–20] discussing the effects of alloying, interface roughness, temperature, etc., on the periods and amplitudes of the oscillations of the interlayer exchange coupling, the results thereof need not be rediscussed in here.

In Fig. 3 the resistivities and the GMR as continued to the real axis are shown. Again pronounced differences between the two types of systems, Fe or Au substrate, can be seen. The resistivities corresponding to the systems with an Fe substrate are almost a factor of 2 bigger than those referring to systems with a Au substrate. Interdiffusion of the third interface, see left half of Fig. 3, clearly increases the resistivity. For large interdiffusion concentrations, the GMR for the two types of systems are about the same (about 25% at $c=0.2$), crucial differences occur in the regime of very small interdiffusion: at $c=0$ the GMR for the spin valve with the Au substrate becomes rather small.

Since—as was already said—a finite value of the imaginary part δ of the Fermi energy mimics finite-temperature

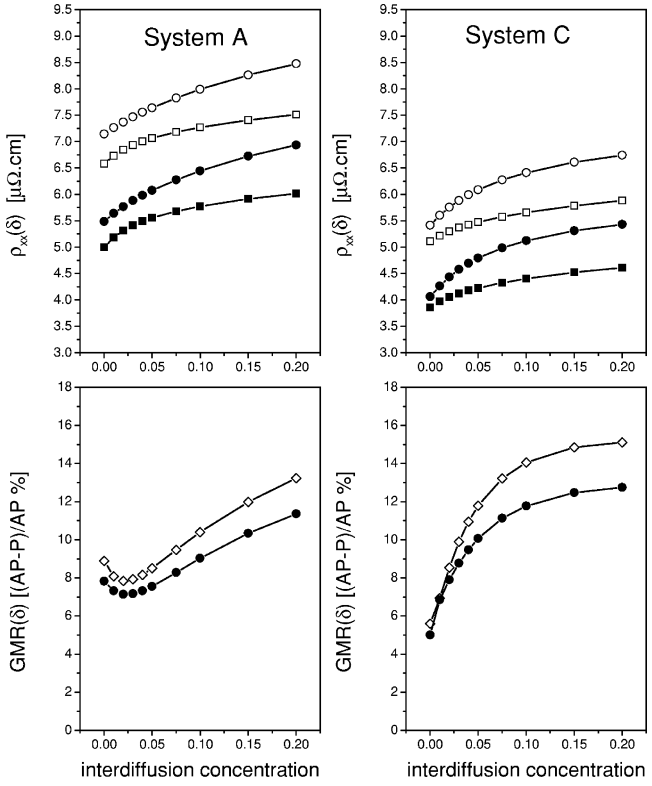

FIG. 4. CIP resistivity and GMR in Fe/Au/Fe multilayers for different values of the imaginary part of the complex Fermi energy. Squares refer to the parallel alignment, circles to the antiparallel alignment; open (full) symbols to an imaginary part of the Fermi energy of 2 (3) mRy. It should be noted that a value of 2 mRy mimickes ''electronic room temperature.''

effects, in Fig. 4 resistivities and the respective GMR are shown for $\delta=2$ (corresponds to about room temperature) and 3 mRy. As to be expected all resistivities increase in magnitude and all GMR values are decreased with increasing δ. Attempting to compare the calculated values for the resistivities with those measured from samples of unknown interdiffusion clearly poses quite a delicate problem. The safest conclusion reduces to the statement that the theoretical and the experimental values are of the same order of magnitude, whereby the theoretical values differ from the experimental ones by a factor of 3–4. Since in the experiment the contacts were attached to the Au parts of the system, i.e., the Au parts served as electron reservoir, it is quite remarkable that the theoretical calculations indeed reflect this experimental detail quite well: the functional behavior of the GMR with respect to interdiffusion, see Fig. 3, shows that for vanishing interdiffusion only system C, see Table I, heads for the experimental GMR value, whereas in a system with Fe leads (systems A and B)—which was not measured—the corresponding GMR value, if experimentally accessible at all, would be much higher, namely by a factor of 3–4.

Using layer-dependent conductivities, see also Eq. (10), allows one to discuss the spatial distribution of the conductivity. It is important, however, to recall that only the sum over all layer-resolved conductivities is well defined. The difference between systems with an Fe substrate and a Au

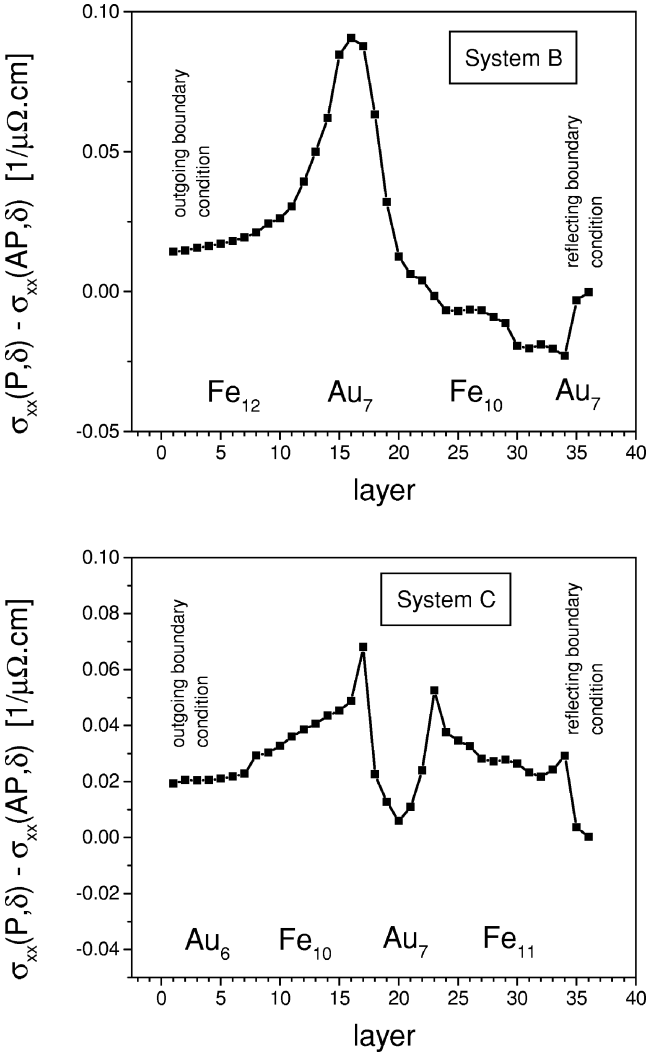

FIG. 5. Layer-resolved difference conductivities corresponding to an imaginary part of the Fermi energy of 2 mRy and an interdiffusion concentration of $c=0.05$.

substrate can be magnified by viewing directly the difference of the layer-resolved conductivities in the parallel and the antiparallel configuration,

$$\Delta\sigma^{i}_{xx}(n;\mathbf{c};\delta)=\sigma^{i}_{xx}(n;\mathbf{c};\mathcal{P};\delta)-\sigma^{i}_{xx}(n;\mathbf{c};\mathcal{AP};\delta). \quad (12)$$

In Fig. 5 an example of these layer-resolved differences is shown, namely as obtained for $\delta=2$ mRy and considering interdiffusion at all Fe/Au interfaces with an interdiffusion concentration of $c=0.05$ (see also Table I). In this figure outgoing boundaries correspond to the matching up with the semi-infinite lead and reflecting boundary conditions to the vacuum (surface side of a free surface). For a discussion of the effect of boundary conditions see also Blaas *et al.*[12] In system B (Fig. 5, top) the main contribution to the magnetoresistance is due to the Au spacer, i.e., the set of Au layers sandwiched between the two magnetic Fe slabs is the main reason for the magnetoresistance in this system. In system C (Fig. 5, bottom) the two magnetic Fe slabs act as spacers, from which again the main contribution to the GMR comes

from. However, one also can see the relevance of the interfaces. It is indeed somewhat surprising, that—at least in these particular systems—the ''spacer'' plays a somewhat more important role than the interfaces. As for both types of systems the spacers are rather thin, confinement effects obviously are of crucial importance.

V. CONCLUSION

It was shown in this paper that *ab initio* calculations of the electric properties of spin valves can be described quite accurately in terms of the spin-polarized fully relativistic Kubo-Greenwood equation in connection with the corresponding screened KKR approach: both resistivities and the GMR are in rather good agreement with the experimental data.

ACKNOWLEDGMENTS

Financial support was provided partially by the RTN network ''Magnetoelectronics'' (Contract No. HPRN-CT-2000-00143), the Austrian Ministry of Science (GZ 45.504), the Austrian Science Foundation (Contract No. W004), and the Hungarian National Science Foundation (OTKA T030240, T038162).

[1] A. Enders, T. L. Monchesky, K. Myrtle, R. Urban, B. Heinrich, J. Kirschner, X.-G. Zhang, and W. H. Butler, J. Appl. Phys. **89**, 7110 (2001).
[2] T. L. Monchesky, B. Heinrich, R. Urban, K. Myrtle, M. Klaua, and J. Kirschner, Phys. Rev. B **60**, 10 242 (1999).
[3] T. L. Monchesky, A. Enders, R. Urban, K. Myrtle, B. Heinrich, X.-G. Zhang, W. H. Butler, and J. Kirscher (unpublished).
[4] P. Weinberger and L. Szunyogh, Comput. Mater. Sci. **17**, 414 (2000).
[5] P. Weinberger, Philos. Mag. B **75**, 509 (1997), e.g., for a discussion of the concept of parent lattices.
[6] C. Uiberacker, J. Zabloudil, P. Weinberger, L. Szunyogh, and C. Sommers, Phys. Rev. Lett. **82**, 1289 (1999); R. H. Hammerling, C. Uiberacker, J. Zabloudil, L. Szunyogh, P. Weinberger, and J. Kirschner, Phys. Rev. B **66**, 052402 (2002).
[7] P. Weinberger, P. M. Levy, J. Banhart, L. Szunyogh, and B. Újfalussy, J. Phys.: Condens. Matter **8**, 7677 (1996).
[8] P. Weinberger, L. Szunyogh, C. Blaas, and C. Sommers, Phys. Rev. B **64**, 184429 (2001).
[9] S. H. Vosko, L. Wilk, and M. Nusair, Can. J. Phys. **58**, 1200 (1980).
[10] C. Blaas, P. Weinberger, L. Szunyogh, P. M. Levy, and C. Sommers, Phys. Rev. B **60**, 492 (1999).
[11] C. Blaas, L. Szunyogh, P. Weinberger, C. Sommers, and P. M. Levy, Phys. Rev. B **63**, 224408 (2001).
[12] C. Blaas, L. Szunyogh, P. Weinberger, C. Sommers, P. M. Levy, and J. Shi, Phys. Rev. B **65**, 134427 (2002).
[13] A. Fuß, S. Demokritov, P. Grünberg, and W. Zinn, J. Magn. Magn. Mater. **103**, L221 (1992).
[14] J. Kudrnovský, V. Drchal, I. Turek, M. Šob, and P. Weinberger, Phys. Rev. B **53**, 5125 (1996).
[15] V. Drchal, J. Kudrnovský, I. Turek, M. Šob, and P. Weinberger, Phys. Rev. B **53**, 15 036 (1996).
[16] J. Kudrnovský, V. Drchal, C. Blaas, I. Turek, and P. Weinberger, Phys. Rev. Lett. **76**, 3834 (1996).
[17] J. Kudrnovský V. Drchal, P. Bruno, I. Turek, and P. Weinberger Phys. Rev. B **54**, R3738 (1996).
[18] J. Kudrnovský, V. Drchal, R. Coehhorn, M. Šob, and P. Weinberger, Phys. Rev. Lett. **78**, 358 (1997).
[19] J. Kudrnovský, V. Drchal, P. Bruno, I. Turek, and P. Weinberger, Phys. Rev. B **56**, 8919 (1997).
[20] V. Drchal, J. Kudrnovský, P. Bruno, P. H. Dederichs, and P. Weinberger, Phys. Rev. B **60**, 9588 (1999).